NANO · MICRO small
www.small-journal.com

A Förster Resonance Energy Transfer-Based Ratiometric Sensor with the Allosteric Transcription Factor TetR

*Thuy T. Nguyen, Margaret Chern, R C. Baer, James Galagan, and Allison M. Dennis**

A recent description of an antibody-free assay is significantly extended for small molecule analytes using allosteric transcription factors (aTFs) and Förster resonance energy transfer (FRET). The FRET signal indicates the differential binding of an aTF–DNA pair with a dose-dependent response to its effector molecule, i.e., the analyte. The new sensors described here, based on the well-characterized aTF TetR, demonstrate several new features of the assay approach: 1) the generalizability of the sensors to additional aTF–DNA–analyte systems, 2) sensitivity modulation through the choice of donor fluorophore (quantum dots or fluorescent proteins, FPs), and 3) sensor tuning using aTF variants with differing aTF–DNA binding affinities. While all of these modular sensors self-assemble, the design reported here based on a recombinant aTF–FP chimera with commercially available dye-labeled DNA uses readily accessible sensor components to facilitate easy adoption of the sensing approach by the broader community.

Förster resonance energy transfer (FRET), the nonradiative transfer of energy from an excited donor fluorophore to an acceptor,[1] has been used for small molecule analyte detection when paired with molecular recognition elements like antibodies,[2,3] aptamers,[4,5] or substrate-binding proteins.[6,7] When fluorescent acceptors are used in addition to the requisite fluorescent donors, changes in the photoluminescence of both the donor and acceptor molecules yield an internally calibrated ratiometric output correlated to analyte concentration.[8] This internal calibration controls for changes in sensor concentration and environmental effects, allowing for more accurate quantification.[8] Furthermore, by exhibiting a change in fluorescent signal that is highly responsive to the change in distance between the donor and acceptor fluorophores, FRET sensors enable homogeneous assays, eliminating the need for tedious and time-consuming washing steps.[9]

In related efforts,[10] we expanded the list of molecular recognition elements suitable for homogeneous FRET assays to include allosteric transcription factors (aTFs), a specific class of substrate-binding protein that binds both DNA and a small molecule effector in discrete protein domains. Here, we describe additional novel sensors using the well-characterized aTF TetR for molecular recognition, modulate the sensor sensitivity using aTF variants that alter the aTF–DNA binding affinities, and demonstrate an additional sensor design with a genetically encoded donor fluorophore. These additional sensors show the generalizability of our approach, while detailing a sensor design more readily adoptable by a wide variety of research groups.

Allosteric transcription factors are regulatory proteins comprising a DNA-binding domain as well as an effector-binding domain able to recognize small molecules with high specificity and selectivity.[11] In the presence of the target analyte, the aTF affinity for its DNA binding sequence is modulated, facilitating the repressor or derepressor regulation of downstream gene expression.[11] The distinct, but interrelated, binding of the aTF to its cognate DNA and effector ligand provides an intrinsic transduction mechanism that we couple to FRET for optical readout.[10] Other previously described substrate-binding protein-based FRET sensors achieved changes in donor–acceptor distance through displacement of a dye-labeled ligand (competitive assay) or conformational changes in the protein.[6,7] Our aTF-based FRET sensors utilize the analyte-responsive unbinding of the donor-labeled aTF and its acceptor-labeled cognate DNA sequence to effect a large change in the donor–acceptor distance. Thus, these FRET sensors eliminate the need to dye-label ligands, which can change their binding behavior,[12] while enabling the substantial signal changes produced through complete dissociation of the donor and acceptor fluorophores (**Figure 1**).

We chose TetR for this study because it is a well-characterized aTF that is used extensively for gene regulation and inducible protein expression in the laboratory setting.[11] The TetR

T. T. Nguyen, Prof. J. Galagan, Prof. A. M. Dennis
Department of Biomedical Engineering
Boston University
Boston, MA 02215, USA
E-mail: aldennis@bu.edu
Dr. M. Chern, Prof. A. M. Dennis
Division of Materials Science and Engineering
Boston University
Boston, MA 02215, USA
R. C. Baer, Prof. J. Galagan
Department of Microbiology
Boston University
Boston, MA 02218, USA
Prof. J. Galagan
National Emerging Infections Diseases Laboratories
Boston University
Boston, MA 02218, USA
The ORCID identification number(s) for the author(s) of this article can be found under https://doi.org/10.1002/smll.201907522.

DOI: 10.1002/smll.201907522

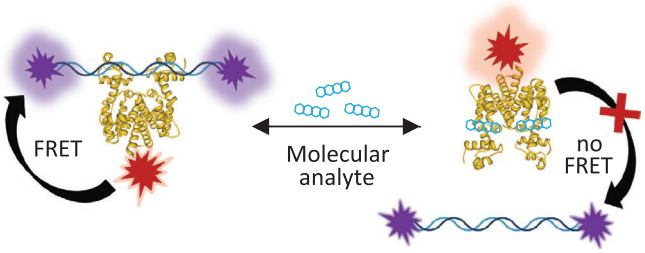

Figure 1. Schematic representation of sensor mechanism. An allosteric transcription factor (aTF) labeled with a donor fluorophore (red) binds its cognate DNA sequence labeled with an acceptor fluorophore (purple). In this bound state, the proximity of the fluorophores promotes Förster resonance energy transfer (FRET) from the donor to the acceptor following photoluminescent excitation of the donor fluorophore. The binding of the aTF effector ligand (aka, the molecular analyte) to the aTF induces a conformational change in the protein, reducing its binding affinity for the DNA. The release of the DNA from the aTF extends the distance between their respective fluorophores, reducing energy transfer, yielding an analyte dose-dependent change in FRET and the donor and acceptor fluorescence intensities. The aTF used here, TetR, is a homodimer with two ligand binding pockets per dimer.[11]

regulatory complex evolved in bacteria to turn on the production of TetA efflux pumps to protect the cells from the antibiotic tetracycline. In microbial systems, the biosynthetic precursor to tetracycline, anhydrotetracycline (aTc), also binds to the repressor TF, TetR, and induces production of the efflux pump shortly before the cell is exposed to the impending influx of tetracycline.[13] As aTc itself is not an antimicrobial agent, its derepressor activity has been effectively harnessed to induce production of proteins encoded by downstream genes in synthetic biology.[14] In the absence of tetracycline or its derivatives, TetR homodimers bind the cognate DNA sequence *tetO* with high affinity (K_D(TetR + *tetO*) ≈ 10^{-10} M).[15] When complexed with magnesium ions, aTc binds to TetR very strongly (K_D (TetR + aTc–Mg^+) ≈ 10^{-12} M).[15,16] This TetR–aTc binding induces a conformational change in TetR, shifting the alpha helices that interact with the major groove of the DNA.[11] This adjustment reduces the affinity of TetR for *tetO* by four orders of magnitude (K_D(TetR–aTc–Mg^+ + *tetO*) ≈ 10^{-6} M).[15] Thus, while TetR binding to both aTc and *tetO* is not mutually exclusive, for practical purposes, the binding of aTc to TetR induces the release of *tetO*.

FRET-based sensors utilizing the TF–DNA binding between TetR class C ($TetR^C$) and the *tetO* oligonucleotide sequence (Table S1, Supporting Information) were developed and characterized for the sensing of aTc, a small molecule analyte that reduces the TF affinity for its cognate DNA.[11,17] In the sensor design, the 19 bp cognate sequence was flanked by 4–5 bp on each side to ensure binding, resulting in a 28 bp DNA oligo. One of the strands was labeled with the FRET acceptor Cy5 on both the 5′ and 3′ ends. A second 28 bp sequence with no affinity for TetR (scrambled sequence) was similarly labeled to act as the negative control (Table S1, Supporting Information).

The choice of donor and acceptor fluorophores is an important factor in the design and overall performance FRET-based devices. We explored differences between using fluorescent proteins (FPs) or quantum dots (QDs) as FRET donors to dye-labeled oligomeric DNA. Each sensor uses Cy5-modified DNA as the FRET acceptor with either a transcription factor–fluorescent protein ($TetR^C$–tdTomato; TF–FP) fusion protein (expressed in *Escherichia coli*) or quantum dot–transcription factor (QD–TF) conjugate as the donor (Figure 1). The QD–Cy5 FRET pair exhibits increased spectral overlap (*J*) between its photoluminescence (PL) emission peak and the Cy5 absorption compared to tdTomato–Cy5 (Figure S1 and Table S2, Supporting Information). The higher quantum yield (QY) of tdTomato compared to the QDs (69% vs 23%), however, results in a larger calculated Förster distance, R_0, for the tdTomato–Cy5 FRET pair than the calculated R_0 for the QD–Cy5 FRET pair (7.4 vs 7.0 nm).

While as-synthesized QDs can exhibit near unity QY,[18] thiolate-based ligands like CL4[19] used to confer water solubility while maintaining a minimal particle size significantly quench the QD photoluminescence due to the introduction of surface trap states.[20,21] Nevertheless, the thin organic coating is desirable both to reduce donor–acceptor distance and to enable histidine-tag-mediated self-assembly of the proteins to the QD surface.[21] Our previous work demonstrated that moderately thick-shelled core/shell/shell QD heterostructures improve the QD quantum yield and brightness in water, while minimizing the distance added between the donor and acceptor molecules for efficient energy transfer.[22] Thus, we utilized core/shell/shell QDs comprising CdSe/4CdS/2ZnS, where the number before the shell composition indicates the number of atomic monolayers that were deposited on the core, coated with a thiolated zwitterionic ligand, CL4.[19] The diameter of the semiconductor QD is 7.6 ± 1.1 nm based on transmission electron microscopy (TEM) (Figure S2, Supporting Information), while dynamic light scattering (DLS) of the water-soluble particles indicates a hydrodynamic diameter of 10 ± 2 nm, showing the minimal increase in size from the CL4 ligand coating.

Despite a smaller Förster distance (R_0) and larger donor–acceptor distance due to the donor size, the QD-based sensor exhibits higher donor fluorophore quenching (68%) than the tdTomato-based sensor (34%), attributable to the multivalency of the nanoparticle platform (**Figure 2**). Specifically, multiple his-tagged TFs self-assemble on the surface of the QD, enabling the binding of multiple acceptor dye-labeled oligos to a single QD donor. Adding multiple acceptor molecules has the benefit of increasing the FRET efficiency compared to a single acceptor at the same donor–acceptor distance.[23,24] Titrating the Cy5–DNA FRET acceptors against the $TetR^C$–tdTomato or QD–$TetR^C$ donors elucidates the donor:acceptor ratio that maximizes energy transfer with the donor concentration adjusted to keep the $TetR^C$ concentration constant at 200 × 10^{-9} M. When the *tetO* sequence is used, we observe the characteristic nonlinear response to increasing acceptor concentration, which is fit to a modified Hill equation (Table S2, Supporting Information).[25] The linear response from the scrambled control is described by Stern–Volmer collisional quenching,[26] demonstrating sequence-specific binding and donor quenching (Figure 2). Inherently, the number of aTFs per donor is unity for the $TetR^C$–tdTomato fusion protein. For QD-based nanoconstructs, his-tagged proteins self-assemble to the QD surface stoichiometrically according to the mixture ratio with a Poissonian distribution of proteins on the QD

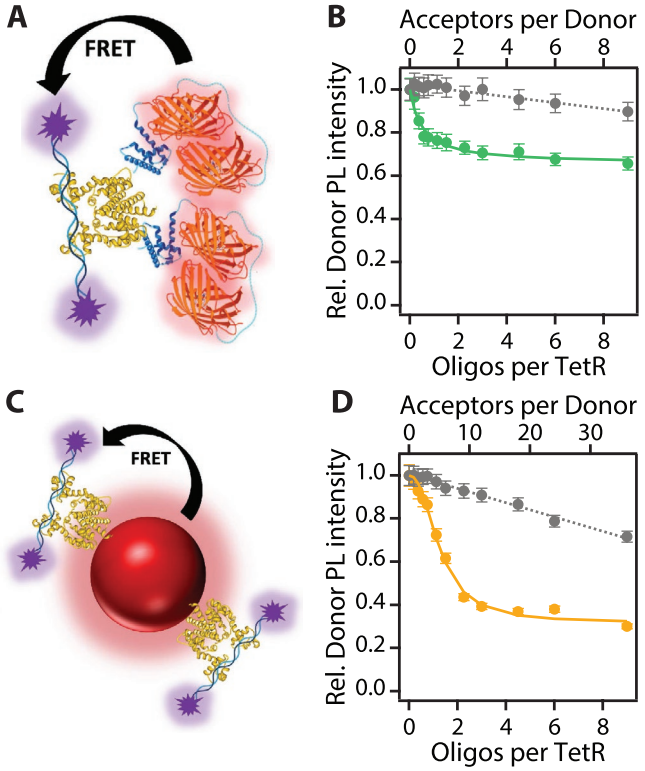

Figure 2. Relative donor photoluminescence (PL) intensity as a function of the amount of Cy5-labeled DNA acceptor for two sensor designs, shown schematically. A,B) $TetR^C$–tdTomato + Cy5–DNA. C,D) QD–$TetR^C$ + Cy5–DNA. $TetR^C$ is displayed in yellow in both panels (A) and (C). In panel (A), tdTomato is in red and an alpha helical linker with sequence AEAAAKEAAAKA is in blue. The bottom axis indicates the ratio of Cy5–DNA to TF ($TetR^C$), while the top axis indicates the ratio of Cy5–DNA to the donor fluorophore (tdTomato or QD) to account for the difference in the stoichiometry. The colored circles are data using the target binding sequence *tetO*; the solid lines are fits to a modified Hill equation. The scrambled sequence (gray) acts as a nonbinding control for collisional quenching and nonspecific binding; the dashed line exhibits the linear fit typical of Stern–Vollmer collisional quenching. Data are means ± standard deviations of $n = 3$.

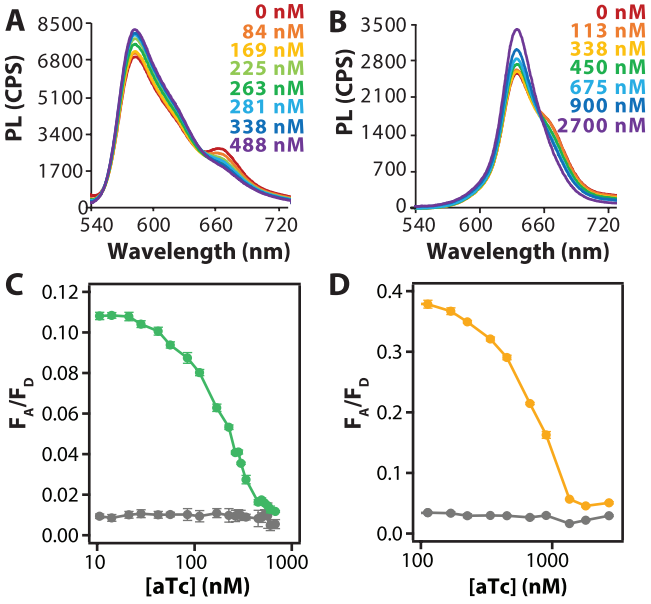

Figure 3. Sensor response to analyte titration. Representative spectral data for the aTc dose-dependent change in photoluminescence intensity for the sensor comprising A) tdTomato–$TetR^C$ + Cy5–DNA or B) QD–$TetR^C$ + Cy5–DNA. Spectra are background-subtracted to eliminate the effects of direct acceptor excitation. A selection of the analyte concentrations is plotted for visual clarity. Ratio of acceptor fluorescence intensity to donor fluorescence intensity as a function of aTc concentration for sensor comprising C) tdTomato–$TetR^C$ + Cy5–DNA or D) QD–$TetR^C$ + Cy5–DNA. The first sensor has a 1:1:3 ratio of tdTomato:TF:DNA, while the second has a 1:4:18 ratio of QD:TF:DNA. tdTomato (200×10^{-9} M) and QD (50×10^{-9} M) concentrations were selected to maintain a constant aTF concentration at 200×10^{-9} M. Data are mean ± standard deviation of $n = 3$.

surface.[27] In early assays, tests of several stoichiometric ratios of protein to QD (i.e., 1, 2, 4, or 6 $TetR^C$ per QD) indicated that the largest response to the Cy5–DNA titration was seen when a sufficient number of TFs were used (i.e., >2) for all QDs to be labeled, but that further increases from 4 to 6 TFs per QD did not substantially improve FRET efficiency (data not shown).

We chose component stoichiometries of 1:1:3 tdTomato:$TetR^C$:Cy5–DNA and 1:4:18 QD:$TetR^C$:Cy5–DNA to maximize FRET efficiency for each sensor for subsequent experiments testing sensor sensitivity to aTc. Photoluminescence spectra measured from sensors with varied concentrations of aTc yielded changes in the ratio between the acceptor PL intensity and donor PL intensity (F_A/F_D). With increasing concentrations of aTc, F_A/F_D values decreased indicating unbinding of the DNA from TetR, resulting in an increase in donor PL and decrease in acceptor PL (**Figure 3**). No changes were observed when aTc was titrated into a solution of nonbinding donor–acceptor pairs. This indicates that the specific recovery of donor PL intensity (and reduction in acceptor PL intensity) is due to TF–DNA unbinding.

To compare the outputs of the two sensors, the F_A/F_D ratios were analyzed to determine the half maximal effective concentration (EC_{50}) and limit of detection (LOD), defined as the aTc concentration yielding an F_A/F_D change greater than three standard deviations from the maximum F_A/F_D measured in the completely bound state. Both the EC_{50} and LOD were found to be lower for the FP–TF-based sensor than that of the QD–TF-based sensor based on either interpolation between points (**Table 1**) or Hill equation fits to the data (Table S3, Supporting Information).

Notably, the FP sensor exhibited improved sensitivity compared to the QD sensor, despite a lower FRET efficiency (i.e., less donor quenching). The inherent 1:1 donor–TF:acceptor–DNA ratio of the FP sensor allows the sensor components to exist in only two states at equilibrium when aTc is present: $TetR^C$–tdTomato and Cy5–DNA are bound or unbound. Thus,

Table 1. Summary of sensor metrics.

Sensor	$TetR^C$–FP	$TetR^C$–QD	$TetR^D$–QD′
EC_{50} [$\times 10^{-9}$ M]	198	670	139
LOD [$\times 10^{-9}$ M]	33.9	93.0	18.1
Dynamic range/width [$\times 10^{-9}$ M]	33.9–596 562	93–1570 1480	18.1–899 881

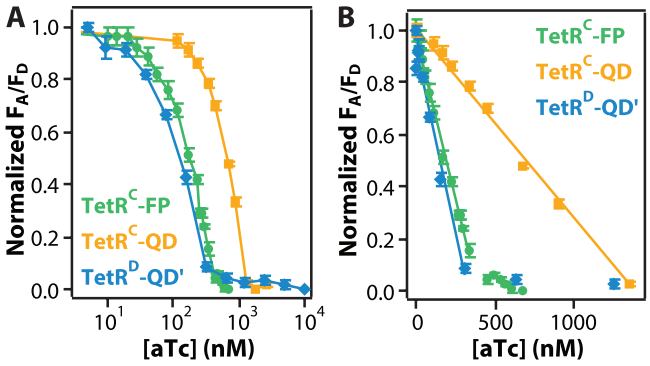

Figure 4. Comparison of ratiometric sensors for aTc. A) Normalized ratio of acceptor and donor fluorescence intensity (F_A/F_D) shows analyte concentration dependence. B) Normalized linear ranges of sensor outputs indicate narrower linear ranges for the more sensitive probes.

for an individual sensor, the binding of aTc switches the sensor state from maximum to minimum FRET. In contrast, the multivalency of the QD sensor enables multiple binding states related to the number of Cy5–DNA acceptors bound (e.g., 0, 1, and 2), requiring multiple TF–DNA unbinding events to transition the sensor between the maximum and minimum FRET states. Accordingly, the multivalency of the QD sensor may reduce its sensitivity at the same concentration of aTF.

To examine the role of TF–DNA affinity on the sensitivity of the sensor, we used TetR class D (TetR^D) in a similar format as the QD–TetR^C sensor. TetR^C and TetR^D are structurally very similar; we confirmed with biolayer interferometry (BLI) that both bind to the *tetO* DNA sequence and exhibit differential binding affinity depending on whether the effector molecule aTc is bound or unbound. TetR^D, however, exhibits an eight-fold lower affinity (higher K_D) for *tetO* (Table S3, Supporting Information). We found that by using TetR^D in place of TetR^C in this sensor, we were able to produce a QD–TF sensor with an LOD and linear range similar to the FP–TF sensor (**Figure 4** and Table 1). The lower affinity of TetR^D for *tetO* results in lower FRET efficiency because fewer dye-labeled *tetO* sequences bind at the same concentrations (Figure S3, Supporting Information). Concomitantly, a lower concentration of aTc induces complete unbinding, yielding a lower LOD. The linear dose responses of the more sensitive sensors are also steeper, exhibiting a more pronounced normalized spectral response to the analyte (Figure 4B). Our results with a progesterone-responsive aTF demonstrate that changes to the DNA binding sequence, which substantially change the aTF–DNA binding affinity, likewise alter the sensitivity of the FRET sensor.[10] These results together demonstrate the tunability of the approach.

Only very recently have aTFs been examined as biomolecular recognition elements for in vitro sensing.[10,28–31] Of the limited number of signal transduction mechanisms explored, only ours utilizes FRET. One homogeneous assay achieved nanomolar sensing using an amplified luminescent proximity homogeneous assay (AlphaScreen).[28] However, this nonratiometric approach requires specialized equipment (a plate reader equipped with a 680 nm laser), commercialized beads that are expensive, and unstable under visible light, and provides a negative output signal.[28,31] Two other assay designs provide only an indirect measure of aTF–DNA binding by amplifying and quantifying (un)bound DNA.[29–31] Using existing methods of DNA detection facilitates incorporation into existing workflows but lacks the advantages of a real-time, homogeneous assay without substantial gains in the LOD or linear dynamic range.[29–31] Our FRET-based sensor maintains the rapidity and convenience of the homogeneous assay, while incorporating a ratiometric output and widely accessible fluorophores to facilitate broader adoption.

As the foundations for aTF-based biosensing are established, there is potential to adapt the sensor platform to the growing number of characterized and optimized analyte-responsive transcription factors. The number and type of identified aTF–analyte pairs are large and diverse.[32–37] Some compounds that can be sensed include toluene,[38] cholesterol,[39,40] parathion[41] (commonly used in insecticides), metabolites like pyruvate,[42] lactate,[43] and mevalonate,[44] and a number of ligands used as gene expression inducers in molecular biology and the synthetic biology community.[45,46] A recent report describes the optimized orthogonal responsivity of 12 aTFs for 12 different small molecules,[46] and other papers describe numerous examples of evolved and mutation-optimized aTFs.[47–53] The potential to identify desired aTFs from prokaryotic sources[10] coupled with new analyte sensitization and optimization through directed evolution and recombinant protein engineering opens the door to using aTFs for sensing of any number of small molecule analytes.

In summary, we have demonstrated the generalizability of our homogeneous FRET assay based on aTFs by applying the approach to a new protein–DNA–analyte system, while also expanding our analysis and characterization of this new class of sensors. The advantages of the approach make it suitable for use beyond our initial demonstration:[10] 1) it is modular, and thereby adaptable to other aTF–DNA pairs responsive to a wide range of small molecules of interest; 2) self-assembly of sensor components in aqueous solution simplifies sensor construction; 3) sensor sensitivity can be modulated through the use of aTFs with different affinities for their corresponding DNA binding sequence; 4) sensor response can be modulated through the choice of FRET donor and its related valency; and 5) the sensing approach is effective using genetically encoded FP–aTF chimeras and commercially available customized dye-labeled oligos, enabling wide adoption of the sensing approach using easily accessible sensor components. This robust and modular homogeneous assay has significant potential for the sensing of small molecule analytes using differential aTF–DNA binding. Our demonstration of multiple homogeneous FRET assay designs using the well-known aTF TetR indicates potential for the immediate implementation of this approach with the many other aTFs that have been identified from nature and are being actively engineered by the synthetic biology community.

Supporting Information

Supporting Information is available from the Wiley Online Library or from the author.

Acknowledgements

The authors acknowledge the helpful discussions and material support afforded by their larger collaborative effort, which includes Mingfu Chen and Dr. Chloé Grazon from the lab of Prof. Mark Grinstaff, Dr. Andy Fan, Prof. Mario Cabodi, and the lab of Prof. Catherine Klapperich. Financial support provided to T.T.N., R.C.B., J.G., and A.M.D. through DARPA grant W911NF-16-C-0044. Financial support for M.C. was provided through the Clare Boothe Luce (CBL) Graduate Fellowship from the Henry Luce Foundation. A.M.D. was supported by the National Institutes of Health National Center for Advancing Translational Sciences through BU-CTSI Grant Number 1KL2TR001411 and National Institute of General Medical Sciences through Grant Number R01GM129437. Thank you to Prof. Douglas Densmore's CIDAR Lab and Evan Appleton for supplying MoClo plasmids and protein design advice. This work was performed in part at the Center for Nanoscale Systems (CNS), a member of the National Nanotechnology Coordinated Infrastructure Network (NNCI), which is supported by the National Science Foundation under NSF award no. 1541959. CNS is part of Harvard University. Biolayer interferometry (BLI) measurements performed at the Biophysical Instrumentation Facility at the Massachusetts Institute of Technology were made possible through support from NIH S10 OD016326. The research team includes members of the Boston University Precision Diagnostics Center, Nanotechnology Innovation Center (BUnano), Photonics Center, Cancer Center, and Neurophotonics Center.

Conflict of Interest

The authors declare no conflict of interest.

Keywords

antibody-free assays, biosensors, Förster resonance energy transfer (FRET), homogeneous assays, molecular recognition, quantum dots, small molecule quantification

Received: December 22, 2019
Published online:

[1] I. L. Medintz, N. Hildebrandt, *FRET–Förster Resonance Energy Transfer: From Theory to Applications*, Wiley, Weinheim, Germany **2013**.
[2] K. D. Wegner, Z. W. Jin, S. Linden, T. L. Jennings, N. Hildebrandt, *ACS Nano* **2013**, *7*, 7411.
[3] M. D. Kattke, E. J. Gao, K. E. Sapsford, L. D. Stephenson, A. Kumar, *Sensors* **2011**, *11*, 6396.
[4] Y. H. Wang, L. Bao, Z. H. Liu, D. W. Pang, *Anal. Chem.* **2011**, *83*, 8130.
[5] F. S. Sabet, M. Hosseini, H. Khabbaz, M. Dadmehr, M. R. Ganjali, *Food Chem.* **2017**, *220*, 527.
[6] I. L. Medintz, E. R. Goldman, M. E. Lassman, J. M. Mauro, *Bioconjugate Chem.* **2003**, *14*, 909.
[7] J. A. Mitchell, J. H. Whitfield, W. H. Zhang, C. Henneberger, H. Janovjak, M. L. O'Mara, C. J. Jackson, *ACS Sens.* **2016**, *1*, 1286.
[8] M. H. Lee, J. S. Kim, J. L. Sessler, *Chem. Soc. Rev.* **2015**, *44*, 4185.
[9] J. Lee, M. B. Brennan, R. Wilton, C. E. Rowland, E. A. Rozhkova, S. Forrester, D. C. Hannah, J. Carlson, E. V. Shevchenko, D. S. Schabacker, R. D. Schaller, *Nano Lett.* **2015**, *15*, 7161.
[10] C. Grazon, R. C. Baer, U. Kuzmanovic, T. Nguyen, M. Chen, M. Zamani, M. Chern, P. Arquino, X. Zhang, S. Lecommandoux, A. Fan, M. Cabodi, C. Klapperich, M. W. Ginstaff, A. M. Dennis, J. E. Galagan, *Nat. Commun.* **2020**, *11*, 1276, https://doi.org/10.1038/s41467-020-14942-5.
[11] L. Cuthbertson, J. R. Nodwell, *Microbiol. Mol. Biol. Rev.* **2013**, *77*, 440.
[12] O. Hegener, R. Jordan, H. Haberlein, *J. Med. Chem.* **2004**, *47*, 3600.
[13] J. R. D. McCormick, E. R. Jensen, S. J. Johnson, N. O. Sjolander, *J. Am. Chem. Soc.* **1968**, *90*, 2201.
[14] R. Bertram, W. Hillen, *Microb. Biotechnol.* **2008**, *1*, 2.
[15] A. Kamionka, J. Bogdanska-Urbaniak, O. Scholz, W. Hillen, *Nucleic Acids Res.* **2004**, *32*, 842.
[16] O. Scholz, P. Schubert, M. Kintrup, W. Hillen, *Biochemistry* **2000**, *39*, 10914.
[17] D. S. Bolintineanu, K. Volzing, V. Vivcharuk, A. Sayyed-Ahmad, P. Srivastava, Y. N. Kaznessis, *J. Chem. Eng. Data* **2014**, *59*, 3167.
[18] Y. Gao, X. G. Peng, *J. Am. Chem. Soc.* **2015**, *137*, 4230.
[19] K. Susumu, E. Oh, J. B. Delehanty, J. B. Blanco-Canosa, B. J. Johnson, V. Jain, W. J. Hervey, W. R. Algar, K. Boeneman, P. E. Dawson, I. L. Medintz, *J. Am. Chem. Soc.* **2011**, *133*, 9480.
[20] I. L. Medintz, H. T. Uyeda, E. R. Goldman, H. Mattoussi, *Nat. Mater.* **2005**, *4*, 435.
[21] A. M. Dennis, D. C. Sotto, B. C. Mei, I. L. Medintz, H. Mattoussi, G. Bao, *Bioconjugate Chem.* **2010**, *21*, 1160.
[22] M. Chern, T. T. Nguyen, A. H. Mahler, A. M. Dennis, *Nanoscale* **2017**, *9*, 16446.
[23] A. R. Clapp, I. L. Medintz, J. M. Mauro, B. R. Fisher, M. G. Bawendi, H. Mattoussi, *J. Am. Chem. Soc.* **2004**, *126*, 301.
[24] M. Chern, J. C. Kays, S. Bhuckory, A. M. Dennis, *Methods Appl. Fluoresc.* **2019**, *7*, 012005.
[25] A. M. Dennis, G. Bao, *Nano Lett.* **2008**, *8*, 1439.
[26] J. R. Lakowicz, *Principles of Fluorescence Spectroscopy*, 3rd ed., Springer, New York, NY **2006**.
[27] T. Pons, I. L. Medintz, X. Wang, D. S. English, H. Mattoussi, *J. Am. Chem. Soc.* **2006**, *128*, 15324.
[28] S. S. Li, L. Zhou, Y. P. Yao, K. Q. Fan, Z. L. Li, L. X. Zhang, W. S. Wang, K. Q. Yang, *Chem. Commun.* **2017**, *53*, 99.
[29] Y. Yao, S. Li, J. Cao, W. Liu, F. Qi, W. Xiang, K. Yang, W. Wang, L. Zhang, *Appl. Microbiol. Biotechnol.* **2018**, *102*, 7489.
[30] J. Cao, Y. Yao, K. Fan, G. Tan, W. Xiang, X. Xia, S. Li, W. Wang, L. Zhang, *Sci. Adv.* **2018**, *4*, eaau4602.
[31] Y. P. Yao, S. S. Li, J. Q. Cao, W. W. Liu, K. Q. Fan, W. S. Xiang, K. D. Yang, D. M. Kong, W. S. Wang, *Chem. Commun.* **2018**, *54*, 4774.
[32] G. Carbajosa, A. Trigo, A. Valencia, I. Cases, *Nucleic Acids Res.* **2009**, *37*, D598.
[33] M. J. Cipriano, P. N. Novichkov, A. E. Kazakov, D. A. Rodionov, A. P. Arkin, M. S. Gelfand, I. Dubchak, *BMC Genomics* **2013**, *14*, 213.
[34] V. Libis, B. Delepine, J. L. Faulon, *Curr. Opin. Microbiol.* **2016**, *33*, 105.
[35] B. De Paepe, G. Peters, P. Coussement, J. Maertens, M. De Mey, *J. Ind. Microbiol. Biotechnol.* **2017**, *44*, 623.
[36] R. Mahr, J. Frunzke, *Appl. Microbiol. Biotechnol.* **2016**, *100*, 79.
[37] R. Fernandez-Lopez, R. Ruiz, F. de la Cruz, G. Moncalian, *Front. Microbiol.* **2015**, *6*, 648.
[38] P. W. Coschigano, B. J. Bishop, *FEMS Microbiol. Lett.* **2004**, *231*, 261.
[39] E. Garcia-Fernandez, F. J. Medrano, B. Galan, J. L. Garcia, *J. Biol. Chem.* **2014**, *289*, 17576.
[40] N. A. T. Ho, S. S. Dawes, A. M. Crowe, I. Casabon, C. Gao, S. L. Kendall, E. N. Baker, L. D. Eltis, J. S. Lott, *J. Biol. Chem.* **2016**, *291*, 7256.
[41] V. Libis, B. Delepine, J. L. Faulon, *ACS Synth. Biol.* **2016**, *5*, 1076.
[42] H. Ogasawara, Y. Ishida, K. Yamada, K. Yamamoto, A. Ishihama, *J. Bacteriol.* **2007**, *189*, 5534.
[43] C. Gao, C. Hu, Z. Zheng, C. Ma, T. Jiang, P. Dou, W. Zhang, B. Che, Y. Wang, M. Lv, P. Xu, *J. Bacteriol.* **2012**, *194*, 2687.
[44] S.-Y. Tang, P. C. Cirino, *Angew. Chem.* **2011**, *123*, 1116.
[45] G. L. Rosano, E. A. Ceccarelli, *Front. Microbiol.* **2014**, *5*, 172.

[46] A. J. Meyer, T. H. Segall-Shapiro, E. Glassey, J. Zhang, C. A. Voigt, *Nat. Chem. Biol.* **2019**, *15*, 196.
[47] N. D. Taylor, A. S. Garruss, R. Moretti, S. Chan, M. A. Arbing, D. Cascio, J. K. Rogers, F. J. Isaacs, S. Kosuri, D. Baker, S. Fields, G. M. Church, S. Raman, *Nat. Methods* **2016**, *13*, 177.
[48] D. Liu, Y. Xiao, B. S. Evans, F. Zhang, *ACS Synth. Biol.* **2015**, *4*, 132.
[49] A. A. Mannan, D. Liu, F. Zhang, D. A. Oyarzun, *ACS Synth. Biol.* **2017**, *6*, 1851.
[50] B. F. Pfleger, D. J. Pitera, J. D. Newman, V. J. Martin, J. D. Keasling, *Metab. Eng.* **2007**, *9*, 30.
[51] D. J. Pitera, C. J. Paddon, J. D. Newman, J. D. Keasling, *Metab. Eng.* **2007**, *9*, 193.
[52] J. K. Rogers, G. M. Church, *Proc. Natl. Acad. Sci. USA* **2016**, *113*, 2388.
[53] F. Zhang, J. M. Carothers, J. D. Keasling, *Nat. Biotechnol.* **2012**, *30*, 354.

